

Tracking studies regarding EMMA FFAG project

F. Méot

DAPNIA & IN2P3

March 2010 - revised from April 2006

Abstract

Based on stepwise ray-tracing methods, the paper shows the results one can expect from ray-tracing means, it gives preliminary results concerning large amplitude dynamics in EMMA, and it establishes basis data and procedures for possible further studies concerning field and alignment defects. With the advantage that the methods is based on realistic magnetic field models, as well as on accurate large amplitude tracking, yielding reliable knowledge of dynamic apertures.

Contents

1	Introduction	3
2	Fields and cell parameters	3
3	Stability limits	6
4	Longitudinal motion	8
4.1	Serpentine	8
4.2	6-D acceleration	9
Appendix		10
A	Zgoubi data file	10
B	Zgoubi data file	10

1 Introduction

EMMA (Electron Model of a Muon Accelerator) [1] is a design of an 10 to 20 MeV electron model of the linear “fixed field alternating gradient” accelerators (FFAG in the following) proposed for the 5 to 20 GeV acceleration of muons in the neutrino factory (NuFact) [2].

The validity of the linear FFAG method needs be proven as concerns, on the one hand the “gutter”, fixed frequency, fast acceleration, and on the other hand the defect tolerances and beam behavior in the presence of multiple resonance crossing inherent to the method. This is the reason for the electron model, a reasonable size experimental machine with reasonable cost.

EMMA is supposed to accelerate an electron beam with large transverse size (several 100π mm.mrad range, normalized). In addition, EMMA will accelerate bunches with large longitudinal emittance, based on a strongly non-linear longitudinal dynamic method (details are given in the following), with non-negligible coupling to transverse motion at large amplitude. From the point of view of the design studies and other optimizations, this raises the question of correct beam dynamics simulations in presence of the non-linearities that affect particle motion : fringe fields, multipolar defects in the lattice combined function (dipole + quadrupole) magnets, large amplitude motion (source of “kinematical terms” in the equations of motion).

For these reasons, one has to resort to stepwise ray-tracing methods in the evaluation of the feasibility of this type of acceleration. This is the goal of the present report, to show the results one can expect from ray-tracing means, to give preliminary results concerning large bunch dynamics in EMMA, and to establish basis data and procedures for possible further studies concerning field and alignment defects. In that, the present study is not very different from earlier ones based on matrix or other drift-kick methods [1, 2], with the advantage that it is based on realistic magnetic field models, as well as on accurate large amplitude tracking, yielding reliable knowledge of dynamic apertures.

2 Fields and cell parameters

EMMA lattice is that proposed for the NuFact muon accelerators [2]. It is based on a unique cell, a quadrupole doublet with two straight sections, one short and one long for, in particular, allowing space for RF cavities (Fig. 1). This lattice has been subject to extensive studies and publications - see the e-model [1] and the CERN NuFact Notes [3] websites for details. The parameters of the design of concern here are summarized in Tab. 1.

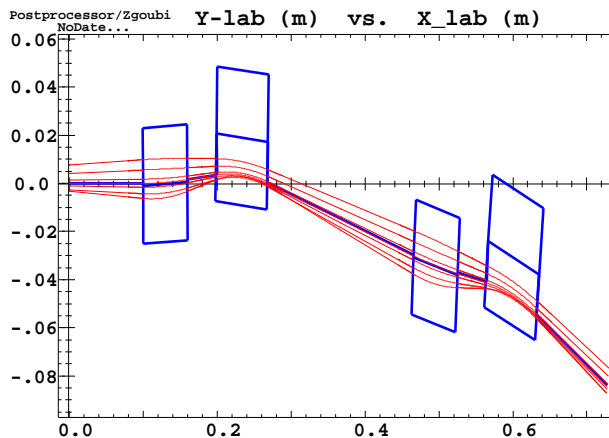


Figure 1: Closed orbits from 10 to 20 MeV (inner to outer trajectories) in a pair of FD cells. RF cavities are located in the long straight.

Table 1: Cell parameters. Bends are treated as straight multipoles with dipole component and gradient, radially displaced.

Optical element	Length (m)	Dipole component (T)	Gradient (T/m)	Radial positioning (m)	Tilt (deg.)
BF	0.06	-0.050721	7.4286	-0.00111	1.4753
BD	0.07	0.074852	-4.6195	0.01708	-5.7610
short drift	0.04				
long drift	0.2				

The focusing (F) and defocusing (D) quadrupoles in the doublet cell are positioned radially so to ensure the bending - and orbit closure - at all energy, they act as combined function dipoles, with alternating bend sign over most of the energy span. The longitudinal phase slip η is minimized, for best use of fixed frequency RF. The small dispersion function entails reduced overall transverse excursion during acceleration (which determines the horizontal optical aperture). Fig. 2 shows the corresponding evolution of magnetic field shape across the cell depending on energy, in the present design. Closed orbit dependence on energy, a specific property of FFAGs, shows a general behavior of outward spiraling from injection to top energy (Figs. 1, 3).

The focusing strength decreases with energy (natural chromaticity, sextupoles are avoided so to obtain large dynamic aperture), with typical behavior as shown in Fig. 4. the largest cell tunes, corresponding to lowest energy, are taken below the half integer, whereas the high energy tunes are kept reasonably high.

The cell geometry also ensures, in the present optics, the working hypothesis of identical time of flight (TOF) at both injection and extraction energies ; on the other hand it results from the longitudinal dynamic that the overall TOF behavior is almost quadratic in momentum difference $\delta \equiv \delta p/p$ (with small higher order dependence in δ), see Fig. 5.

Figs. 3-5 show the behavior of the linear machine parameters in presence of, or without fringe fields. The change in vertical tune due to non-zero fringe field extent, is weak, and however can be recovered from matrix methods by using appropriate extent parameter (f) in the focusing term $(z'/z) = -\tan(w)/\rho + f/(6\rho^2 \cos(w))$ (w = wedge angle, ρ = curvature radius). The change in closed orbit positioning (Fig. 3) is correlated to a change in length and TOF, however weak as seen in Fig. 5.

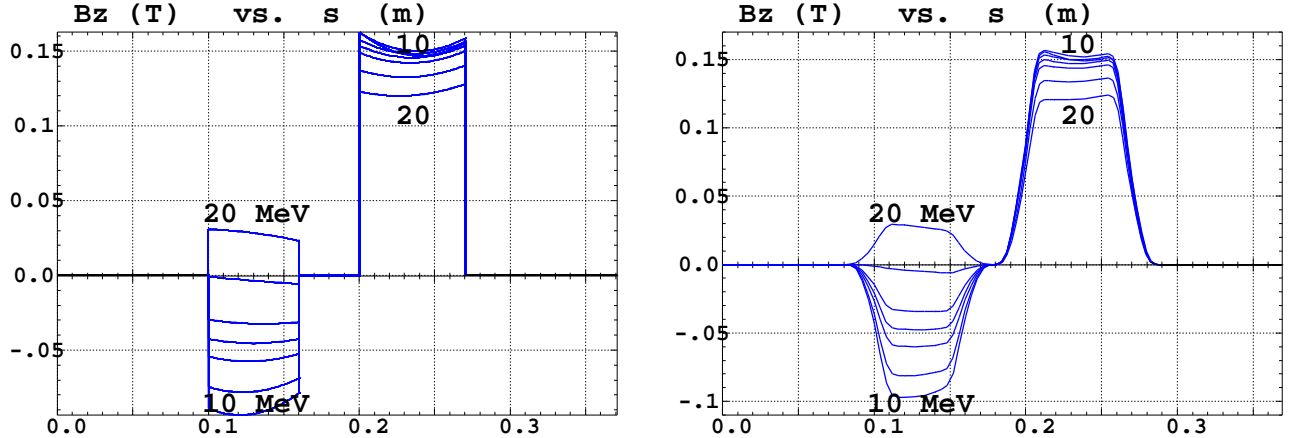


Figure 2: Field on closed orbits along the cell, at various energies, in the sharp-edge (left) or fringe field (right) magnet model.

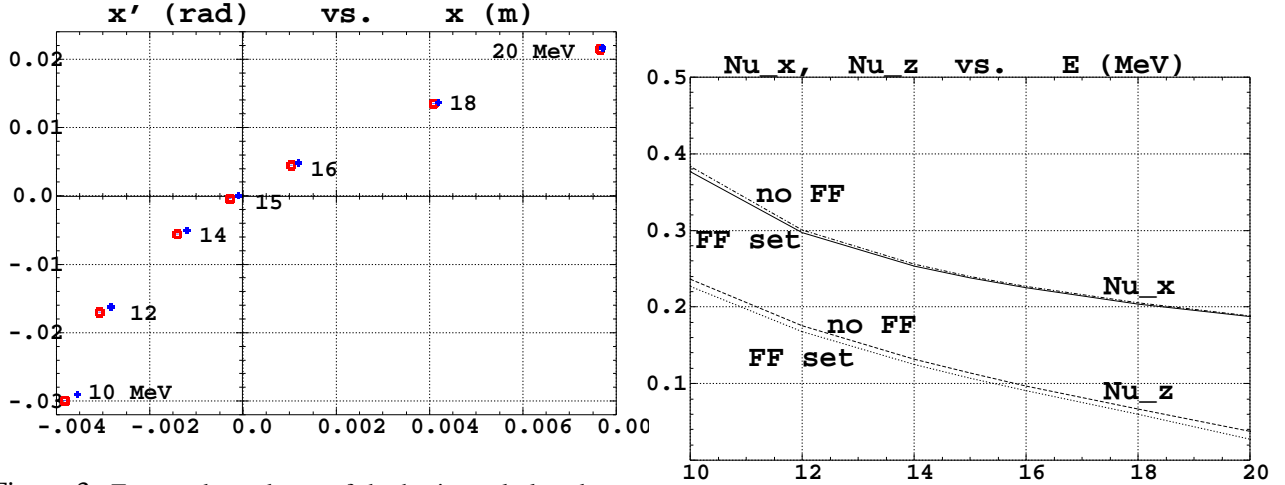


Figure 3: Energy dependence of the horizontal closed orbits in (x, x') phase space, as observed at the center of the long drift, in the case of sharp-edge (squares) or fringe field (crosses) magnet model.

Figure 4: Cell tunes as a function of energy.

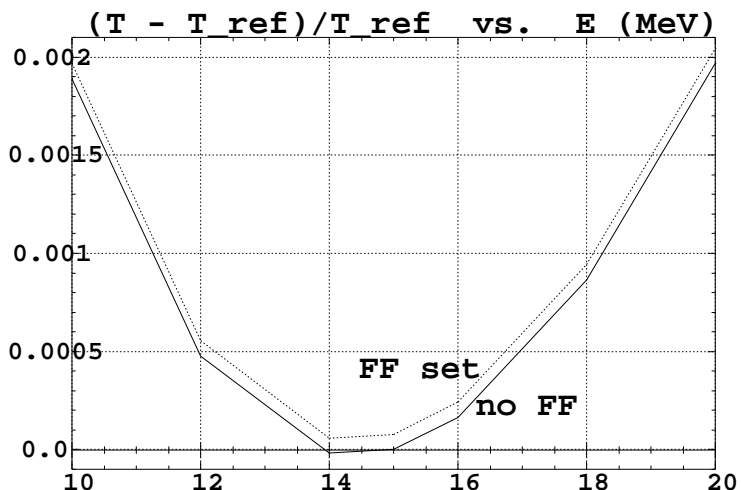


Figure 5: $(T - T_{\text{Ref}})/T_{\text{Ref}}$ as a function of energy.

3 Stability limits

Fig. 6 shows the limit horizontal phase space trajectories at various energies, in case of pure horizontal motion, or including quasi-zero z motion, with or without fringe fields. The presence of arbitrarily small z motion substantially decreases the DA. The presence of fringe fields with 4-D motion tends to increase the DA, in case of coupled motion ; examination of tunes vs. amplitude shows that it could be correlated to a different behavior of the amplitude detuning.

The fact that the invariants shown in Fig. 6 are very thin gives confidence in the symplectic behavior of the integration. In particular, an increase of initial particle position by about a % results in the particle being kicked off (lost), without showing any fuzzy behavior.

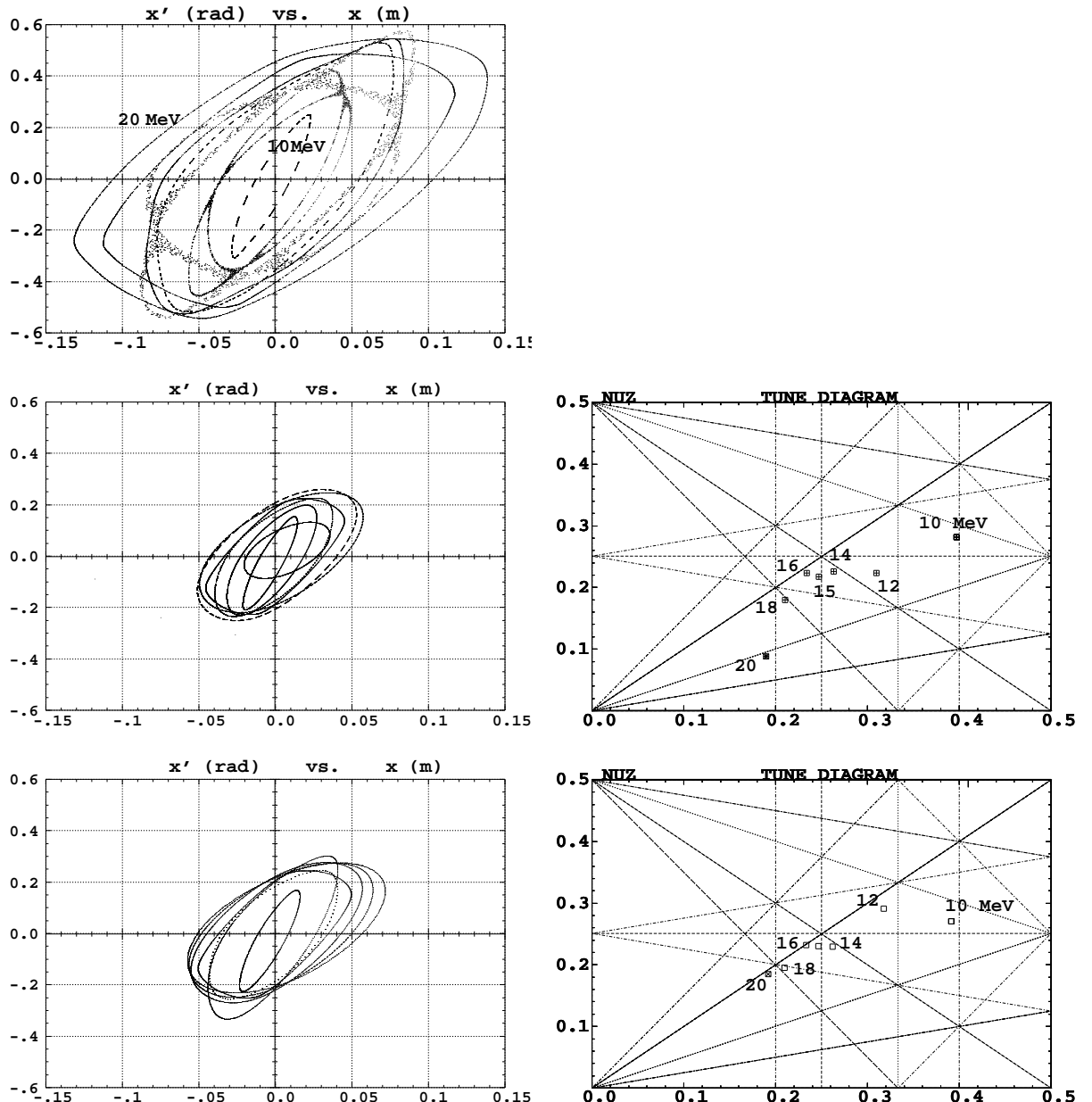


Figure 6: 2-D motion (x, x'), 2000-cell stability limits, with about 5% precision in x , at 10, 12, 14, 15, 16, 18 and 20 MeV (from inner to outer invariant on left graph), and cell tunes at stability limits (resonance lines up to 5th order are represented).

Top : pure horizontal motion, no fringe fields. Middle : in presence of very small z motion, no fringe fields. Bottom : in presence of very small z motion, fringe fields set.

4 Longitudinal motion

4.1 Serpentine

Acceleration of elliptical rings, zero transverse emittance. The channel is not perfectly symmetric, wider at the top. The bunch ellipse is positioned in phase at start (close to π) so as to accelerate from 10 to 20 MeV. The ellipse is tilted (its long axis approximately tangent to the H=Cte line) so as to minimize its deformation. Data details in App. A.

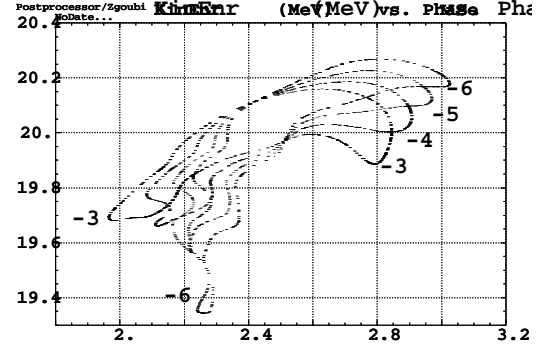
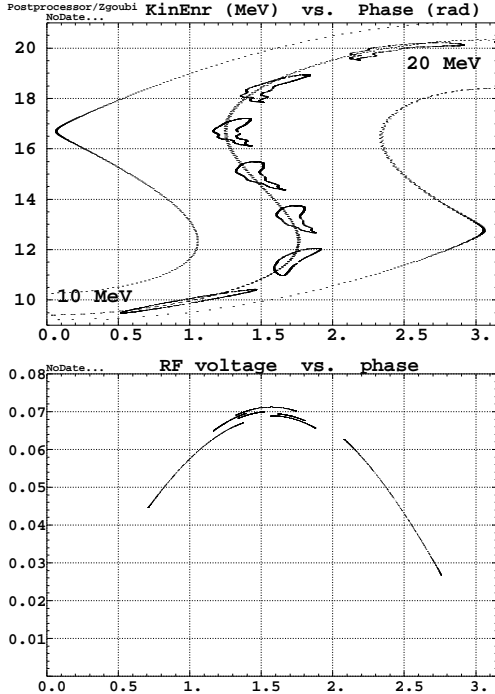


Figure 7: Acceleration of elliptical rings (zero transverse emittances) from about 10 to about 20 MeV in 150 cavity passes. Ellipses are represented each 25 cavity passage. Three particular trajectories show the separatrix and the bunch cog. Voltage : 70 kV peak, RF freq. : 1.3552 GHz. The right plot shows possibilities of optimization of the final longitudinal bunch shape, for instance here by varying the initial ellipse tilt, $-6 \leq \alpha_l \leq -3$.

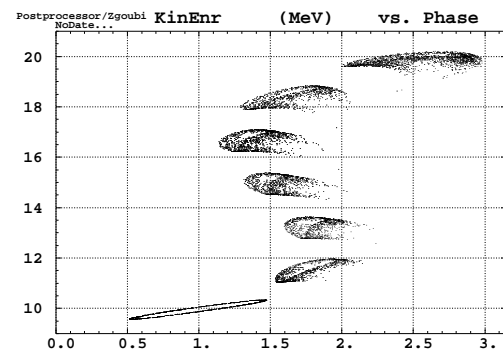
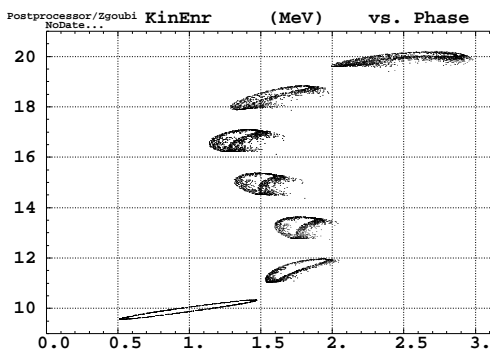


Figure 8: The sensible effect of launching a bunch with non-zero transverse size. Left : $\beta\gamma\epsilon_x/\pi \approx 1.4$ mm, right : $\beta\gamma\epsilon_x/\pi \approx 2.8$ mm. $\epsilon_z = 0$ in both cases.

4.2 6-D acceleration

Working hypothesis : one cavity every 3 other cell, 80 kV per cavity, $f_{RF} = 1.356$ GHz. The top energy is attained in about 130 pass in the cavities. Data details in App. B.

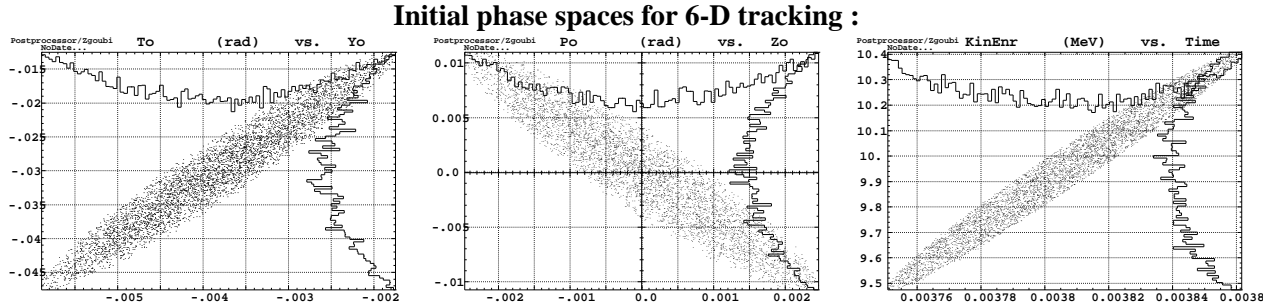


Figure 9: 2000 particle with initial conditions $\epsilon_{x,z} \approx 70 10^{-6}\pi$ m.rad, and $\epsilon_l \approx 0.25 10^{-4}\pi$ eV.s (± 0.125 ns, ± 0.2 MeV).

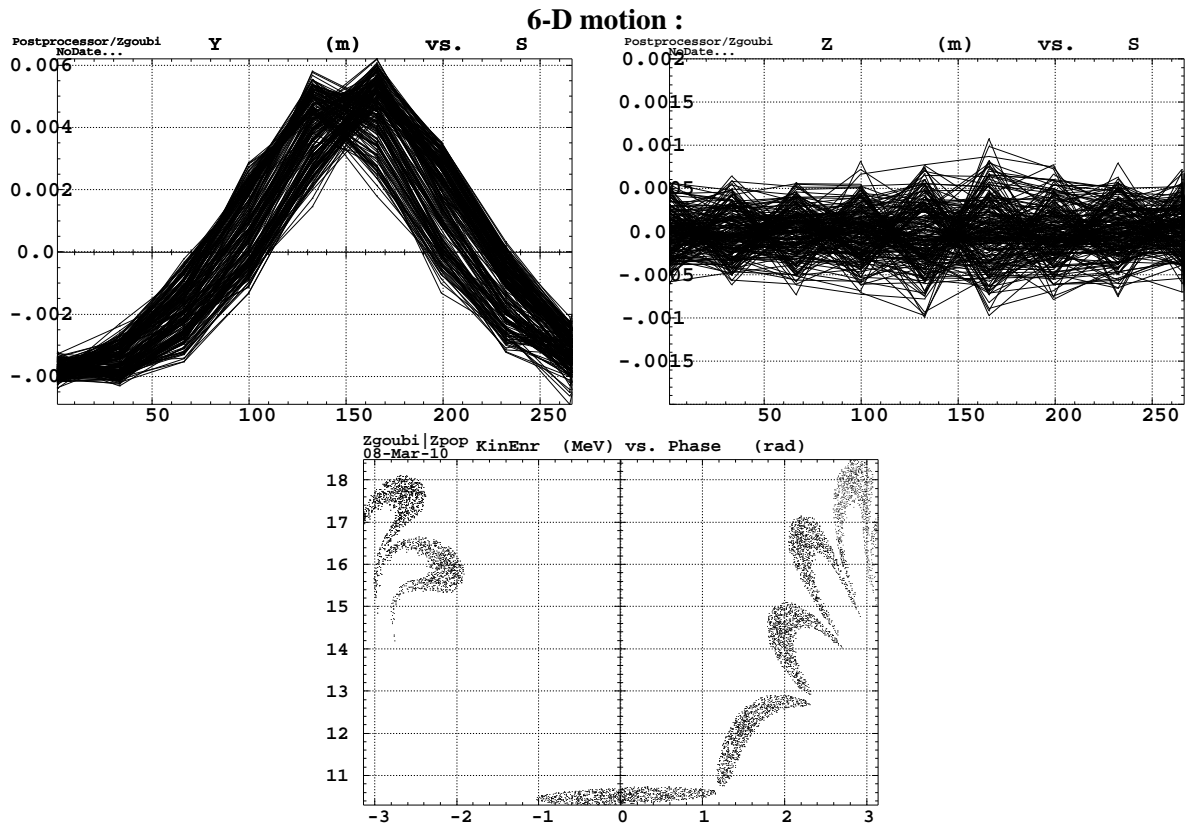


Figure 10: A 5000 particle bunch with initial conditions of Fig. 9 (100 π transverse, 0.12ns \times ± 0.1 eV longitudinal) is accelerated. No fringe fields.

Top, left and right : resp. x-s and z-s during acceleration, observed at cavities. Bottom : longitudinal phase-space.

APPENDIX

A Zgoubi data file

Data used to get the “serpentine”, Sec. 4.1.

```

Test Scott's Fixed Length Lattice
'MCOBJET'
+5.171103865921708e+01      15MeV
3
500
3 3 3 3 2 2
-.382658616E-2 -2.99901128E-2  0.00 0.0  3.3e-2 +0.67 '0'
-1.601153   .197173   .5e-38  4
1.172341   .282063   .5e-38  4
-5 3 2E-4 -.7 .70001
123456 234567 345678
'PARTICUL'
0.51098982 1.60217653e-19 0.0 0.0 0.0
'FAISTORE'
b_zgoubi.fai  CAV
25
'MARKER'    BEG
'DRIFT'     DD1
10
'CHANGREF'
0 -0.1111304250932937 1.47531616464
'MULTIPO'  QF
0
6 2.208947037893755 -5.072134730870179e-01 1.6409348483 0 0 0 0 0 0
0. 0. 2. 1.1 1.00 1.00 1.00 1.00 1.00 1. 1. 1. 1.
4 .1455 2.2670 -.6395 1.1558 0. 0. 0.
0. 0. 2. 1.1 1.00 1.00 1.00 1.00 1.00 1. 1. 1. 1.
4 .1455 2.2670 -.6395 1.1558 0. 0. 0.
#50|10|50 step
1 0 0 0
'CHANGREF'
0 0.1111304250932937 1.47531616464
'DRIFT'    DQ
4
'CHANGREF'
0 1.707551921352993 -5.7610304504
'MULTIPO'  QD
0
7 3.294530758285338 7.485217218484019e-01 -1.52191811761 0 0 0 0 0 0
0. 0. 2. 1.1 1.00 1.00 1.00 1.00 1.00 1. 1. 1. 1.
4 .1455 2.2670 -.6395 1.1558 0. 0. 0.
0. 0. 2. 1.1 1.00 1.00 1.00 1.00 1.00 1. 1. 1. 1.
4 .1455 2.2670 -.6395 1.1558 0. 0. 0.
#200|10|200 step
1 0 0 0
'CHANGREF'
0 0.1111304250932937 1.47531616464
'DRIFT'    DQ
4
'CHANGREF'
0 1.707551921352993 -5.7610304504
'MULTIPO'  QD
0
7 3.294530758285338 7.485217218484019e-01 -1.52191811761 0 0 0 0 0 0
0. 0. 2. 1.1 1.00 1.00 1.00 1.00 1.00 1. 1. 1. 1.
4 .1455 2.2670 -.6395 1.1558 0. 0. 0.
0. 0. 2. 1.1 1.00 1.00 1.00 1.00 1.00 1. 1. 1. 1.
4 .1455 2.2670 -.6395 1.1558 0. 0. 0.
#250|10|250 step
1 0 0 0
'CHANGREF'
0 -1.707551921352993 -5.7610304504
'DRIFT'    DD2
10
'DRIFT'    DD1
10
'CHANGREF'
0 -0.1111304250932937 1.47531616464
'MULTIPO'  QF
0
6 2.208947037893755 -5.072134730870179e-01 1.6409348483 0 0 0 0 0 0
0. 0. 2. 1.1 1.00 1.00 1.00 1.00 1.00 1. 1. 1. 1.
4 .1455 2.2670 -.6395 1.1558 0. 0. 0.
0. 0. 2. 1.1 1.00 1.00 1.00 1.00 1.00 1. 1. 1. 1.
4 .1455 2.2670 -.6395 1.1558 0. 0. 0.
#50|10|50 step
1 0 0 0
'CHANGREF'
0 0.1111304250932937 1.47531616464
'DRIFT'    DQ
4
'CHANGREF'
0 1.707551921352993 -5.7610304504
'MULTIPO'  QD
0
7 3.294530758285338 7.485217218484019e-01 -1.52191811761 0 0 0 0 0 0
0. 0. 2. 1.1 1.00 1.00 1.00 1.00 1.00 1. 1. 1. 1.
4 .1455 2.2670 -.6395 1.1558 0. 0. 0.
0. 0. 2. 1.1 1.00 1.00 1.00 1.00 1.00 1. 1. 1. 1.
4 .1455 2.2670 -.6395 1.1558 0. 0. 0.
#50|10|50 step
1 0 0 0
'CHANGREF'
0 -1.707551921352993 -5.7610304504
'DRIFT'    DQ
4
'CHANGREF'
0 0.1111304250932937 1.47531616464
'DRIFT'    DQ
4
'CHANGREF'
0 1.707551921352993 -5.7610304504
'MULTIPO'  QD
10
'DRIFT'    DD2
10
'DRIFT'    DD1

```

B Zgoubi data file

Data used for 6-D acceleration in Sec. 4.2.

```

Test Scott's Fixed Length Lattice
'MCOBJET'
+5.171103865921708e+01      15MeV
3
2000
3 3 3 3 2 2      15
-.382658616E-2 -2.99901128E-2  0.00 0.0 0.0 +0.6772144197220 '0'
-1.601153   .197173   .5e-6  1
1.172341   .282063   .5e-6  1
0. 3 .5E-3 1. 4
123456 234567 345678
'PARTICUL'      5
0.51098982 1.60217653e-19 0.0 0.0 0.0
'FAISTORE'      7
b_zgoubi.fai
#50|10|50 step
1 0 0 0
'CHANGREF'
0 -0.1111304250932937 1.47531616464
'MULTIPO'  QF
0
6 2.208947037893755 -5.072134730870179e-01 1.6409348483 0 0 0 0 0 0
0. 0. 2. 1.1 1.00 1.00 1.00 1.00 1.00 1. 1. 1. 1.
4 .1455 2.2670 -.6395 1.1558 0. 0. 0.
0. 0. 2. 1.1 1.00 1.00 1.00 1.00 1.00 1. 1. 1. 1.
4 .1455 2.2670 -.6395 1.1558 0. 0. 0.
#50|10|50 step
1 0 0 0
'CHANGREF'
0 0.1111304250932937 1.47531616464
'DRIFT'    DQ
4
'CHANGREF'
0 1.707551921352993 -5.7610304504
'MULTIPO'  QD
0
6 2.208947037893755 -5.072134730870179e-01 1.6409348483 0 0 0 0 0 0
2. 1.1 1.00 1.00 1.00 1.00 1.00 1. 1. 1. 1.
4 .1455 2.2670 -.6395 1.1558 0. 0. 0.
2. 1.1 1.00 1.00 1.00 1.00 1.00 1. 1. 1. 1.
4 .1455 2.2670 -.6395 1.1558 0. 0. 0.
#1000|10|100 step
1 0 0 0
'CHANGREF'
0 0.1111304250932937 1.47531616464
'DRIFT'    DQ
4
'CHANGREF'
0 1.707551921352993 -5.7610304504
'MULTIPO'  QD
15
'DRIFT'    DD2
10
'DRIFT'    DD1

```

```

2. 1.1 1.00 1.00 1.00 1.00 1.00 1. 1. 1. 1. 1.
4 .1455 2.2670 -.6395 1.1558 0. 0. 0.
0 0 0 0 0 0 0 0 0
#150|10|150 step
1 0 0 0
'CHANGREF'
0 -1.707551921352993 -5.7610304504
'DRIFT' DD2
10
'DRIFT' DD1
10
'CHANGREF'
0 -0.1111304250932937 1.47531616464
'MULTIPOLE' QF
0
6 2.208947037893755 -5.072134730870179e-01 1.6409348483 0 0 0 0 0 0 0 0
2. 1.1 1.00 1.00 1.00 1.00 1. 1. 1. 1. 1.
4 .1455 2.2670 -.6395 1.1558 0. 0. 0.
2. 1.1 1.00 1.00 1.00 1.00 1. 1. 1. 1. 1.
4 .1455 2.2670 -.6395 1.1558 0. 0. 0.
0 0 0 0 0 0 0 0 0
#50|10|50 step
1 0 0 0
'CHANGREF'
0 0.1111304250932937 1.47531616464
'DRIFT' DQ
4
'CHANGREF'
0 1.707551921352993 -5.7610304504
'MULTIPOLE' QD
0
7 3.294530758285338 7.485217218484019e-01 -1.52191811761 0 0 0 0 0 0 0 0
2. 1.1 1.00 1.00 1.00 1.00 1. 1. 1. 1. 1.
4 .1455 2.2670 -.6395 1.1558 0. 0. 0.
2. 1.1 1.00 1.00 1.00 1.00 1. 1. 1. 1. 1.
4 .1455 2.2670 -.6395 1.1558 0. 0. 0.
0 0 0 0 0 0 0 0 0
#50|10|50 step
1 0 0 0
'CHANGREF'
0 -1.707551921352993 -5.7610304504
'DRIFT' DD2
10
'DRIFT' DD1
10
'CHANGREF'
0 -0.1111304250932937 1.47531616464
'MULTIPOLE' QF
0
6 2.208947037893755 -5.072134730870179e-01 1.6409348483 0 0 0 0 0 0 0 0
2. 1.1 1.00 1.00 1.00 1.00 1. 1. 1. 1. 1.
4 .1455 2.2670 -.6395 1.1558 0. 0. 0.
2. 1.1 1.00 1.00 1.00 1.00 1. 1. 1. 1. 1.
4 .1455 2.2670 -.6395 1.1558 0. 0. 0.
0 0 0 0 0 0 0 0 0
#50|10|50 step
1 0 0 0
'CHANGREF'
0 0.1111304250932937 1.47531616464
'DRIFT' DQ
4
'CHANGREF'
0 1.707551921352993 -5.7610304504
'MULTIPOLE' QD
0
7 3.294530758285338 7.485217218484019e-01 -1.52191811761 0 0 0 0 0 0 0 0
2. 1.1 1.00 1.00 1.00 1.00 1. 1. 1. 1. 1.
4 .1455 2.2670 -.6395 1.1558 0. 0. 0.
2. 1.1 1.00 1.00 1.00 1.00 1. 1. 1. 1. 1.
4 .1455 2.2670 -.6395 1.1558 0. 0. 0.
0 0 0 0 0 0 0 0 0
#50|10|50 step
1 0 0 0
'CHANGREF'
0 -1.707551921352993 -5.7610304504
'DRIFT' DD2
10
'FAISCEAU'
'CAVITE'
7
1.1050041 1.356e9 ORBIT LENGTH for BORO 15MeV, RF freq
80e3 0. VLT, relative phase of 1st cavity
'MARKER' CAV
'REBELOTE'
240 0.2 99
'END'

```

References

- [1] <http://hepunx.rl.ac.uk/uknf/wp1/emodel/>.
- [2] <http://www.cap.bnl.gov/mumu/project/ISS/>.
- [3] <http://slap.web.cern.ch/slap/NuFact/NuFact/NFNotes.html>.
- [4] E-model with RF systems at 1.3 GHz, E. Keil, CERN NuFact Note 146 (2005).
- [5] O CAMELOT ! A Memoir Of The MURA Years (Section 7.1), F.T.Cole, Proc. Cycl. Conf, April 11, 1994 ; FFAG particle accelerators, K.R. Symon et als., Phys.Rev. Vol.103-6, 1837-1859, 1956.
- [6] Zgoubi users' guide, F. Méot and S. Valero, FERMILAB-TM-2010 (1997). See also, NIM A 427 (1999) 353-356.